

# Thermomechanical Processing of Inconel 718 by Shock-Wave Deformation

MARC A. MEYERS AND R. NORMAN ORAVA

The response of Inconel 718 nickel-base alloy to thermomechanical processing (TMP) utilizing a 510 Kbar planar shock wave was evaluated. The results were compared with those of conventional TMP by cold rolling to 19.1 pct reduction in thickness; this provided a generalized (or effective) strain equivalent to the transient shock strain. Instead of deformation in the solution treated condition, the inclusion of a predeformation, partial aging step in an optimized TMP schedule led to the greatest improvements in strength, stress-rupture life, and low-cycle fatigue life. The mechanical behavior was correlated with substructure and microstructure. Predeformation aging inhibits thermal recovery during final aging and produces a uniform dispersion of  $\gamma''$  precipitates. On a generalized (or effective) strain basis, conventional TMP by cold rolling produces higher strengths than shock TMP due to a higher dislocation density in the former. This suggests that maximum shear strain is a better basis of comparison. Since dislocation substructure is the primary contributor to property modification of Inconel 718 by TMP, the effective service temperature of thermomechanically processed material is limited to 1200°F (649°C), irrespective of the method of working.

THE synergistic action of thermal and mechanical treatments—termed thermomechanical processing (TMP) or treatment (TMT)—can be an effective means of strengthening nickel-base alloys at ambient and intermediate temperatures.<sup>1-4</sup> Studies<sup>2,5-7</sup> of the response of Inconel 718 to conventional TMP have shown that the strength can be increased at temperatures up to 1200°F (649°C) but the stress-rupture life is impaired in the 1000°F (538°C) to 1200°F (649°C) range. In an effort to overcome this problem, and to gain further improvements in overall properties, an investigation was carried out to evaluate the response of Inconel 718 to TMP when conventional working is replaced by deformation imparted during the propagation of a high-amplitude, explosively-generated, shock wave. That this approach could prove to be successful was suggested by the favorable preliminary results for Udimet 700.<sup>8</sup> The study includes a comparison with the effects of thermal treatment and of TMP by cold rolling, optimization of heat treatment parameters, and an interpretation of the mechanical behavior in terms of structural features.

Shock TMP is rendered an attractive processing technique either if conventional deformation is not feasible or if shock TMP yields improvements over those attainable by conventional TMP. The stringent requirements currently being placed on superalloys in critical applications could tend to override some of the adverse considerations involving the economy of explosive fabrication.

## EXPERIMENTAL PROCEDURE

Inconel 718 sheet, of thickness 0.093 in. (2.36 mm), was obtained from Active Alloys, Inc., in a solution

MARC A. MEYERS is Associate Professor, Seção de Ciência dos Materiais, Instituto Militar de Engenharia, Pça. Ten. Tibúrcio, Urca, Rio de Janeiro, RJ, Brasil. R. NORMAN ORAVA is Professor, Department of Metallurgical Engineering, South Dakota School of Mines and Technology, Rapid City, SD 57701.

Manuscript submitted May 12, 1975.

annealed condition [1750°F (954°C)] meeting AMS 5596C. The material was taken from two different heats, I and II, with chemical analyses given in Table I. Table II provides details of the two standard heat treatment schedules, designated 1 and 2, which are recommended for Inconel 718.

Deformation was imparted either by cold rolling to

Table I. Chemical Analyses for Inconel 718, Wt Pct

Element	Heat I	Heat II
Al	0.48	0.51
B	0.003	0.004
C	0.07	0.04
Cb + Ta	5.18	5.13
Co	0.39	0.19
Cr	18.47	17.98
Cu	0.04	0.03
Fe	17.86	20.05
Mn	0.09	0.08
Mo	3.06	3.00
Ni	53.38	51.79
P	0.004	0.005
Si	0.08	0.09
S	0.006	0.005
Ti	0.89	1.10

Table II. Thermal and Thermomechanical Processing Schedules for Inconel 718

Schedule Code	Solution Treatment	Aging Sequence
1 and (TMP-1)*	1750°F (954°C), 1 h, AC (+ cold work*)	1325°F (718°C), 8 h, FC to 1150°F (621°C), Total 18 h, AC
2 and (TMP-2)	1950°F (1066°C), 1 h, AC (+ cold work)	1400°F (760°C), 10 h, FC to 1200°F (649°C), Total 20 h, AC
3 and (TMP-3)	1750°F (954°C), 1 h, AC	1300°F (704°C), 4 h, AC; (+ cold work) 1250°F (677°C), 8 h, FC in 1 h to 1150°F (621°C), Total 18 h, AC

\*TMP-1R, 2R, 3R: cold rolled to 91.1 pct reduction in thickness.

TMP-1S, 2S, 3S: shock loaded to 510 Kbar.

19.1 pct reduction in thickness, or by explosive shock loading to a peak pressure of 510 Kbar. For TMP utilizing Schedule 1 and 2 heat treatments, *i.e.* Schedules TMP-1 and TMP-2, cold working was performed in the solution treated condition, followed thereafter by the standard aging sequence indicated in Table II. Schedules TMP-1R and TMP-1S, for example, apply then to conventional and shock TMP, respectively. The discussion for Schedule 3, and TMP-3 where straining is performed after a partial aging treatment, is reserved for a later section.

A planar shock wave of peak pressure 510 Kbar and 1- $\mu$ s duration was introduced at ambient temperature by the parallel impact with the specimen of a 3 mm thick copper driver plate. This was accelerated explosively by means of a parallel-plate plane-wave generator, using DuPont Detasheet C plastic sheet explosive. Care was taken to properly momentum trap the specimen to prevent spallation, and to minimize the effect of lateral release waves. Further details of the experimental technique and methods for calculating driver-plate velocity, peak pressure, and the equation of state for Inconel 718 may be found elsewhere.<sup>9,10</sup> Cold rolling was performed at ambient temperature by a succession of passes, with approximately 0.5 pct reduction per pass.

The comparison of the properties of material processed by conventional and shock TMP was effected at an equivalent effective (or generalized) strain. A shock pressure of 510 Kbar provided a transient effective true strain of 24 pct. This is equivalent to 19.1 pct reduction in thickness by cold rolling. However, it is emphasized that the residual reduction in thickness by shock loading is only about 2 pct.

Tensile tests at all temperatures were conducted in air with a floor-model 10,000 lb. capacity Instron universal testing machine at a nominal strain rate of  $3 \times 10^{-4} \text{ S}^{-1}$ . Stress-rupture properties were evaluated in air under constant-load conditions by means of a Satec creep machine. The results of tensile and stress rupture tests are the average of two tests. The area under a true stress-true strain curve to fracture was taken as a measure of material toughness, and was termed toughness index. Low-cycle fatigue (LCF) tests were carried out in the Instron by stress-cycling in

tension-tension at a frequency of 2 cycles/min (0.03 Hz); LCF specimens were flat, double-edge notched ( $K_t = 2$ ).

For transmission electron microscopy in a Philips EM 200 electron microscope operated at 100 KV, 3 mm diam discs were thinned electrolytically to perforation in a solution containing 33 vol pct concentrated  $\text{HNO}_3$  and 67 vol pct  $\text{CH}_3\text{OH}$ . Fractography was conducted in an AMR 900 scanning electron microscope.

Differential thermal analysis experiments were conducted in a Deltatherm II apparatus. The standard insert, consisting of four sample/reference pair wells and a monitor well were immersed in a protective argon atmosphere. The thermal effects from the references and samples were added by means of a thermopile connection. The heating rate was equal to  $10^\circ\text{C}/\text{min} \pm 0.25^\circ\text{C}/\text{min}$ . Samples weighing 0.1 to 0.2 gm were cut to size with a high-speed cut-off machine; subsequent electropolishing for 2 min served to remove any surface damage.

## RESULTS OF PRELIMINARY TMP

A preliminary assessment of the response of Inconel 718 to shock TMP was made by combining cold working with the standard heat treatment conditions, Schedules 1 and 2. The effectiveness of shock TMP is demonstrated in Table III (Heat I) from which it can be seen that strength levels at room temperature and  $1200^\circ\text{F}$  ( $649^\circ\text{C}$ ) are raised more than by conventional TMP. The influence of shock TMP on the ductility parameters is mixed, with total elongation decreasing, consistent with lower work-hardening rates, while the reductions in area remain approximately the same or increase slightly. The latter is reflected in some improvement in toughness, as manifested by the values for toughness index.

Table IV shows that the Schedule TMP-1 did not produce any substantial improvement in the stress-rupture properties at  $1200^\circ\text{F}$  ( $649^\circ\text{C}$ ); this is in agreement with previous findings.<sup>11</sup> Conversely, using Schedule 2 thermal treatments, conventional TMP raised the stress-rupture life by 50 pct, and shock TMP by 150 pct, with minimal effect on rupture ductility.

Table III. Tensile Properties of Thermally and Thermomechanically Processed Onconel 718 for the Standard Schedules, Heat I

TMP Schedule Code	0.2 Pct YS (MN/m <sup>2</sup> )	UTS (MN/m <sup>2</sup> )	Elongation, Pct	RA, Pct	Ductile Fracture Stress (MN/m <sup>2</sup> )	Toughness Index (m - MN/m <sup>3</sup> )
(a) Room Temperature						
1-Undeformed	1,274	1,440	20.0	37.9	2,053	794
1-Rolled	1,408	1,468	9.0	33.1	1,977	680
1-Shocked	1,441	1,472	5.7	38.9	2,178	896
2-Undeformed	1,120	1,311	19.5	34.2	1,895	632
2-Rolled	1,141	1,334	13.2	34.6	1,964	663
2-Shocked	1,260	1,377	6.7	34.3	2,008	691
(b) $1200^\circ\text{F}$ ( $649^\circ\text{C}$ )						
1-Undeformed	1,042	1,114	3.5	17.3	1,322	224
1-Rolled	1,134	1,186	4.3	8.5	1,328	107
1-Shocked	1,156	1,203	1.8	16.8	1,438	240
2-Undeformed	919	1,023	4.8	15.4	1,190	177
2-Rolled	991	1,073	11.4	20.3	1,188	248
2-Shocked	1,040	1,122	9.0	18.3	1,221	228

Table IV. Stress-Rupture Properties and Minimum Creep Rates of Thermally and Thermomechanically Processed Inconel 718 for the Standard Schedules

TMP Schedule	Heat	$\dot{\epsilon}$ min, Pct/h	Elongation, Pct	RA, Pct	Rupture, Life, h
(a) 1200°F/110 Ksi (649°C/758 MN/m <sup>2</sup> )					
1-Undeformed	I	0.037	0.9	11.1	15.7
1-Rolled	I	0.046	1.4	5.7	16.0
1-Shocked	I	0.036	0.9	5.7	9.8
(b) 1200°F/105 Ksi (649°C/724 MN/m <sup>2</sup> )					
2-Undeformed	II	0.0075	2.8	15.1	147.3
2-Rolled	II	0.0038	2.9	10.4	224.5
2-Shocked	II	0.0040	3.7	13.6	380.2

### RESULTS OF MODIFIED TMP SCHEDULE

While the results obtained in the above exploratory investigation were encouraging, neither of the two schedules responded in an entirely satisfactory manner to shock TMP. The 1200°F (649°C) rupture life of Schedule TMP-1S material was 50 pct lower than for Schedule 1, and the tensile strength levels achieved by the application of Schedule TMP-2S were still below those due to Schedule 1, without deformation. It was felt that adjustments in the processing parameters could lead to further property improvements. Therefore, an attempt was made to optimize the thermal treatment conditions to be used in conjunction with deformation.

#### Optimization Procedure

One approach to optimization was suggested by the work of Uy et al.<sup>7</sup> They showed that cold hydrostatic extrusion of Inconel 718 was more effective when deformation was imparted in a partially aged condition. Further evidence supporting a predeformation aging step was provided by Conserva et al.<sup>12</sup> Upon thermomechanically processing 7075 aluminum alloy, the best properties evolved when mechanical deformation was both preceded and succeeded by precipitation treatments. In their opinion, the predeformation aging process introduced a fine, uniform distribution of precipitates which then acted as growth centers during post-deformation aging. Without such nuclei, the second phase would nucleate heterogeneously at dislocations, producing a nonuniform distribution and extensive denuded zones.

Since it is known that  $\gamma''$  can precipitate heterogeneously in Inconel 718,<sup>13,14</sup> the optimization of the heat treatments was based in large part on its response to predeformation aging. Thus, the following sequence was examined: solution anneal + partial age + cold work + final age.

No attempt was made to depart from the solution treatment given to the as-received material, *i.e.*, 1750°F (954°C), since it provides an ASTM grain size of 6 to 8 and the best combination of rupture properties.<sup>15,16</sup> In the optimization phase, deformation was limited to cold rolling (19.1 pct reduction) because of the large number of samples required. The predeformation aging temperature ranged from 1000°F (538°C) to 1400°F (760°C) in 100°F (56°C) increments, for times

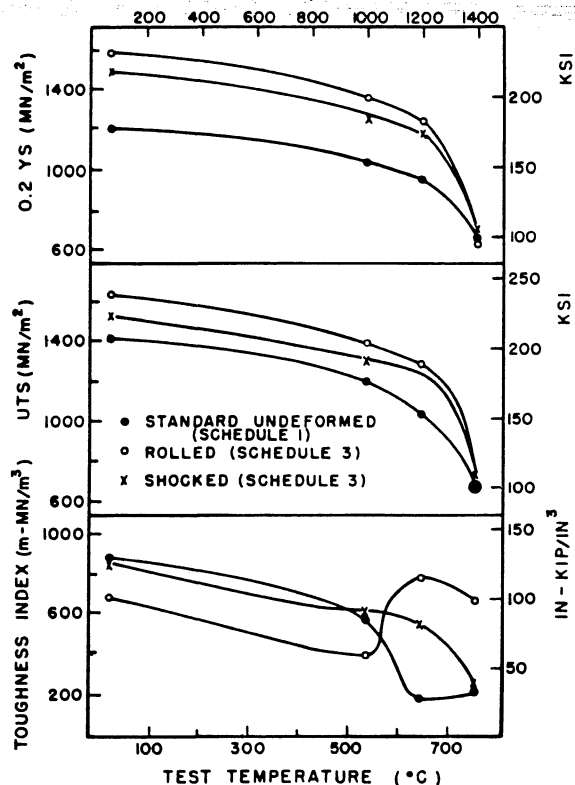


Fig. 1—Influence of optimized TMP Schedule 3 on the strength and toughness of Inconel 718.

of 4 and 8 h. Final single-step aging treatments ranged in temperature from 1000°F (538°C) to 1400°F (760°C) in 100°F (56°C) increments, for times of 4, 8, and 12 h.

However, the hardness data were not sensitive enough to provide a clear distinction among the best predeformation conditions, and the postdeformation aging times. Consequently, ambient temperature and 1200°F (649°C) tensile and stress-rupture tests were conducted in order to further screen the thermal treatments. Taking this into account, it was concluded that the most suitable TMP schedule, optimized on the basis of thermal treatments, is that listed as Schedule TMP-3 in Table II where cold rolling or shock loading is inserted between the 1300°F (704°C) and 1250°F/1150°F (677°C/621°C) aging treatments.

The room and elevated temperature mechanical behavior of Schedule TMP-3 material then was characterized.

#### Tensile Behavior

The strength levels attained through the predeformation aging route (Schedule TMP-3) were significantly higher than those reached by working solution annealed material (Schedules TMP-1 and TMP-2). The effect of temperature on the tensile strengths of TMP-3 material are compared in Fig. 1 with that of material processed thermally according to standard Schedule 1. Strength values are consistently greater, at testing temperatures up to and including 1200°F (649°C), after conventional TMP than after shock TMP. As expected for a process centered around the effects of a deformation substructure, the strengthening gained by TMP disappears at 1400°F (760°C). However, this is not serious since Inconel 718 is designed for intermediate tem-

perature service, in the vicinity of 1200°F (649°C). The effect of TMP-3 on toughness and ductility is more diverse, as seen from Figs. 1 and 2; if these were the only criteria, the choice of one method of working over another would be dictated by the service temperature. At 1200°F (649°C), cold rolling provides the better combination of tensile properties, whereas below 1200°F (649°C), shock TMP is preferable because of superior ductility and toughness.

At this point, the merits of Schedule TMP-3 relative to Schedules TMP-1 and TMP-2 warrant further consideration. Since two heats were used in the investigation a comparison of percentage differences within the same heat was thought to be the most valid one. The TMP Schedules are compared to standard Schedules 1 and 2 in Table V. For each comparison material from the same heat was used in the TMP and standard

Schedule. Thus, the following comparisons are presented:

Schedules TMP-1R and TMP-1S vs Schedule 1

(Heat I)

Schedules TMP-2R and TMP-2S vs Schedule 2

(Heat II)

Schedules TMP-3R and TMP-2S vs Schedule 1

(Heat II).

#### Creep and Stress-Rupture Behavior

Constant-load stress-rupture tests were conducted at 1000°F (538°C) and 1200°F (649°C), at applied stress levels of 170 Ksi (1172 MN/m<sup>2</sup>) and 110 Ksi (758 MN/m<sup>2</sup>).

The optimized TMP schedule led to a dramatic increase in the 1000°F (538°C) rupture life of Inconel 718, as shown by the data in Table VI, without jeopardizing ductility as measured by reduction in area. Elongation to rupture, however, suffers a sharp decline after shock TMP. The enhancement of rupture life persisted up to 1200°F (649°C), with minimal changes in overall ductility. The relative effect of shock and conventional processing is illustrated graphically in Figs. 3 and 4.

Table V. Percentage Change in Tensile Properties of Inconel 718 due to TMP Relative to Standard Thermal Treatments

Processing Schedule Comparison	Heat	0.2 Pct YS	UTS	Elongation	RA	Toughness Index
(a) Room Temperature						
TMP-1R vs 1	I	+10.5	+2.0	-54.8	-12.8	-14.4
TMP-1S vs 1	I	+13.1	+2.2	-71.8	+2.5	+12.8
TMP-2R vs 2	II	+1.9	+1.8	-32.2	-1.3	+5.0
TMP-2S vs 2	II	+12.6	+5.0	-65.5	+0.2	+9.5
TMP-3R vs 1	II	+31.2	+14.7	-71.6	-24.2	-21.6
TMP-3S vs 1	II	+23.4	+7.4	-72.5	-7.4	-0.7
(b) 1200°F (649°C)						
TMP-1R vs 1	I	+8.8	+6.5	+8.0	-50.7	-52.4
TMP-1S vs 1	I	+10.9	+8.0	-53.8	-2.5	+6.9
TMP-2R vs 2	II	+7.8	+4.8	+137.9	+31.7	+40.3
TMP-2S vs 2	II	+13.2	+9.7	+87.9	+18.6	+29.4
TMP-3R vs 1	II	+29.3	+22.0	+26.4	+155.5	+307.3
TMP-3S vs 1	II	+23.2	+17.1	-36.9	+94.7	+187.3

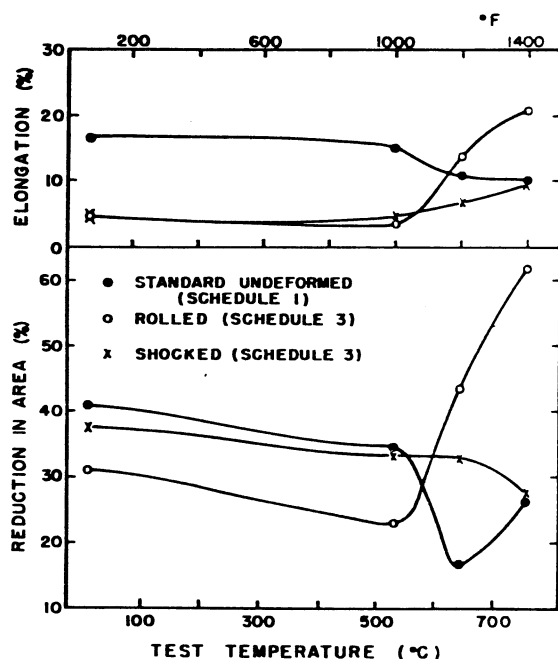


Fig. 2—Influence of optimized TMP Schedule 3 on the ductility of Inconel 718.

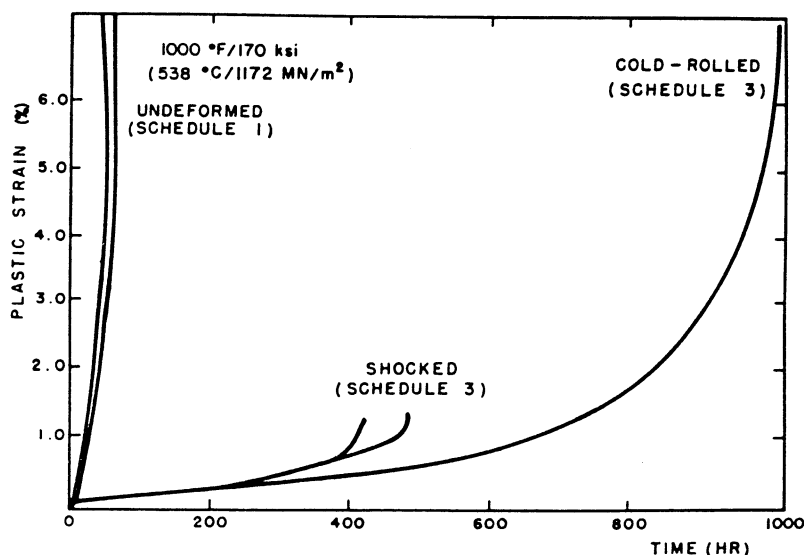
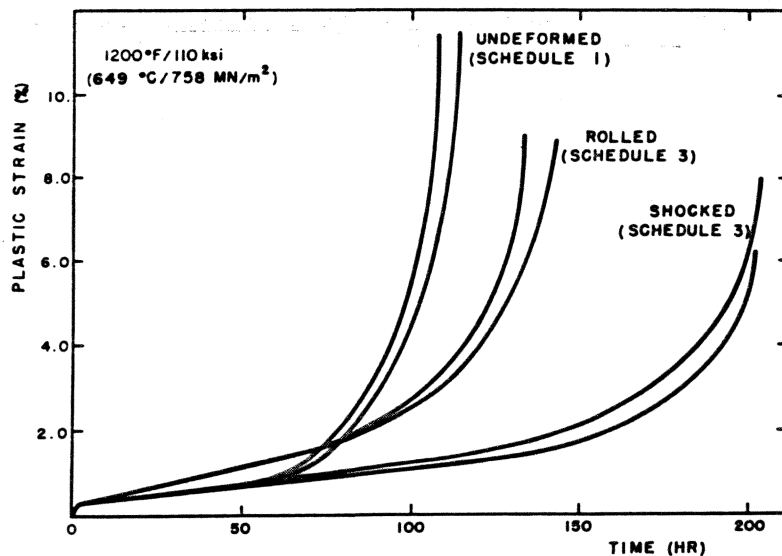


Fig. 3—Constant-load creep curves at 1000°F (537.8°C) for Inconel 718 (TMP Schedule 3).

Fig. 4—Constant-load creep curves at 1200°F (648.9°C) for Inconel 718 (TMP Schedule 3).



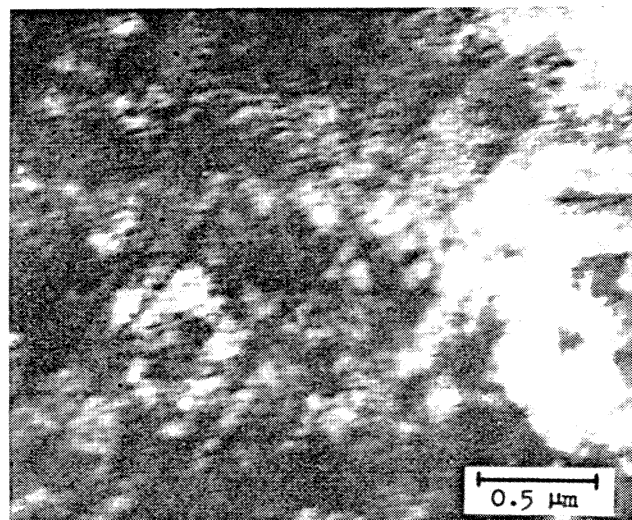
#### Low-Cycle Fatigue Behavior

The major purpose of the LCF tests, conducted at ambient temperature and 1200°F (649°C) was to demonstrate that the improvement in strength and rupture life do not compromise LCF behavior. From the results in Table VII, it is evident that this was not only achieved, but also that LCF life was increased, independent of the method of cold working.

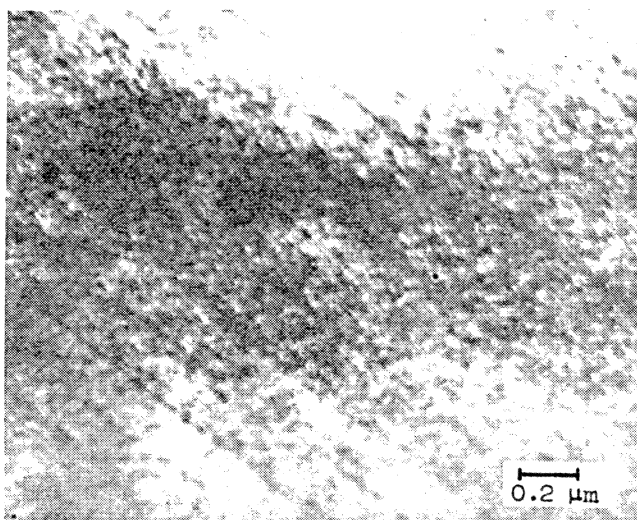
#### Response to Double Shocking

The maximum shock pressure which can be applied reasonably to a material is limited by several factors including the adiabatic temperature rise, maintenance of specimen structural integrity, specimen retrieval, and physical size of charge (*i.e.* environmental factors and explosive facility capacity). The major governing criterion is the second one, since any bending, spallation, microcracking, surface damage, etc must be avoided. A 500-Kbar shock wave in this material would be expected to yield transient and residual temperatures of 536°F (280°C) and 279°F (137°C), respectively. Thus, there is still some latitude for pressure increase without significant *in situ* substructure recovery or aging. Moreover, samples can be propelled into water, as was done in the present investigation, in order to minimize the effects of postshock impact and the residual temperature rise. The duration of the transient heating is controlled by the pulse duration. When all of the factors are taken into consideration, the 500-Kbar region is a reasonable upper limit for the applied shock pressure. However, one can introduce additional shock-strain by multiple shock loading.

A double-shock treatment was given to Inconel 718 in conjunction with the Schedule 3 thermal treatment. The peak pressures were 400 and 510 Kbar, respectively, which provided a total transient true strain of 45 pct. The room-temperature yield strength (Table VIII) increased from 218.1 Ksi (1504 MN/m<sup>2</sup>) for single-shocked material, to 238.6 Ksi (1645 MN/m<sup>2</sup>). The improvement in strength is still noticeable at 1200°F (649°C).



(a)



(b)

Fig. 5—Substructure Effects of shock TMP (TEM of thin foils): (a) Schedule TMP-2S; (b) Schedule TMP-3S.

**Table VI. Stress-Rupture Properties and Minimum Creep Rates of Inconel 718 Processed According to Schedule TMP-3 (Heat II)**

TMP Schedule	$\dot{\epsilon}$ min, Pct/h	Elongation, Pct	RA, Pct	Rupture Life, h
(a) 1000°F/170 Ksi (538°C/1172 MN/m <sup>2</sup> )				
Sch. 1 (Ht. II)	0.079	12.3	22.0	42.7
TMP-3R	0.0020	7.0	17.5	1022.8
TMP-3S	0.0035	1.8	21.2	457.8
(b) 1200°F/110 Ksi (649°C/758 MN/m <sup>2</sup> )				
Sch. 1 (Ht. II)	0.0080	11.3	24.2	111.2
TMP-3R	0.019	8.7	27.2	146.8
TMP-3S	0.0090	7.1	29.3	201.6

**Table VII. Low-Cycle Fatigue Life of Inconel 718 Processed According TMP-3 (Heat II; Mean Values Underlined)**

Test Temperature, °F	Cyclic Stress (MN/m <sup>2</sup> )	No. of Cycles to Failure		
		Sch. 1 (Ht. II)	TMP-3R	TMP-3S
70	724 ± 586	3071	3123	3832
		3351	4544	3734
		<u>3211</u>	<u>3834</u>	<u>3783</u>
1200	552 ± 414	408	979	1071
		895	1385	1060
		843	<u>1182</u>	<u>1066</u>
		<u>715</u>		

## INTERPRETATION AND DISCUSSION

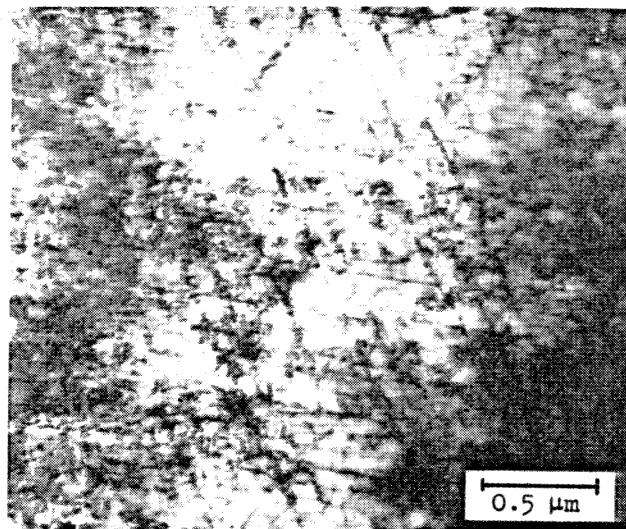
In an attempt to develop a better understanding of the factors responsible for the TMP-induced modification of the properties of Inconel 718, a number of different structure-related characteristics were examined, including: grain morphology; deformation substructure; work-hardening behavior; annealing response; long-term microstructural stability; and fracture modes.

### Grain Morphology

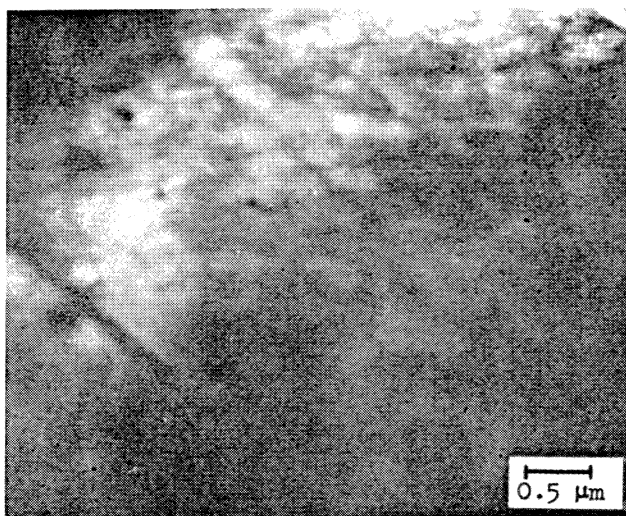
It is generally appreciated that the small residual dimensional changes in workpieces subjected to planar shock waves are not conducive to significant changes in the shape of grains. The grain sizes and their changes were measured along the three principal axes of deformation-processed specimens. The isotropy in grain size characteristic of the solution annealed material was maintained after shocking. Conversely, cold rolling introduced changes in shape consistent with the 19.1 pct reduction in thickness. While this does not establish incontrovertibly the absence of preferred orientation in the shocked material, it strongly suggests that texturing is minimal relative to the cold-rolled state.

### Deformation Substructure

Optical microscopy and TEM revealed that planar slip characterized both methods of cold working; slip bands persisted after post deformation aging treatments. The major observable strain-rate dependent feature of the deformation substructure was the slip-band spacing. Slip-band separations in as-shocked



(a)



(b)

**Fig. 6—Substructure effects of conventional TMP (TEM of thin foils): (a) Schedule TMP-2R; (b) Schedule TMP-3R.**

and shock TMP material were very regular and averaged about 0.1 μm. Mean values of 0.10 μm, 0.10 μm, and 0.14 μm were measured in as-shocked specimens prior to aging to the TMP-2S condition (Fig. 5(a)), in the TMP-2S condition itself and in the TMP-3S condition (Fig. 5(b)), respectively. Conversely, planar slip was much less uniformly distributed in conventionally-processed material, with band spacings varying among different schedules and within any given thin foil. The minimum slip band spacing of 0.12 μm was found in the as-rolled TMP-2R material (Fig. 6(a)). Band separations were generally larger in fully-processed TMP-2R and in TMP-3R samples (Fig. 6(b)), with values as high as 0.6 μm and 1.0 μm, respectively.

### Precipitate Distribution

Because of its relatively high misfit with the lattice, it was reasonable to suppose that γ'' precipitates preferentially at slip bands upon aging after deformation (Refs. 3 and 4). Indeed, such heterogeneous nucleation



Table VIII. Influence of Double-Shocking for the Optimized Schedule (3) on the Tensile Properties of Inconel 718 (Heat II)

Test Temperature, °F	0.2 Pct YS (MN/m <sup>2</sup> )	UTS (MN/m <sup>2</sup> )	Elongation, Pct	RA, Pct	Ductile Fracture Stress (MN/m <sup>2</sup> )	Toughness Index (m - MN/m <sup>3</sup> )
70	1,645	1,675	4.3	28.7	2,077	630
1200	1,279	1,302	7.2	40.3	1,502	717

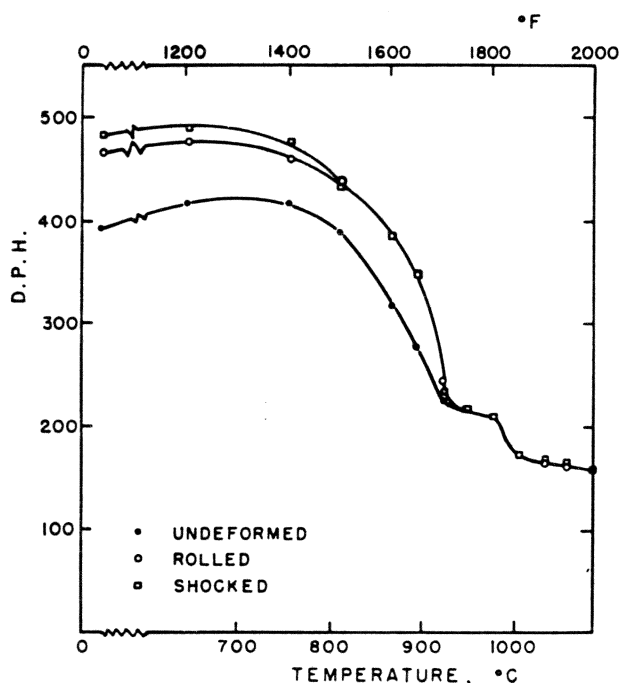


Fig. 7—Isochronal annealing (1 h) curves for undeformed, rolled and shock-loaded Inconel 718 with a predeformation aging of 1300°F (704.4°C)/4 h (Schedule 3).

of  $\gamma''$  was confirmed for Schedule TMP-2 by TEM; this Schedule has the highest aging temperature and largest  $\gamma''$  precipitates. In the other Schedules, the combination of a high dislocation density and small precipitate size interfered with similar observations and precluded confirmation. The immobilized planar dislocation arrays can act as significant obstacles to further slip.

#### Annealing Response

The response of Inconel 718 to thermal recovery of the deformation substructure was monitored by three techniques: hardness measurements, optical metallography, and differential thermal analysis. Fig. 7 shows the results for as-deformed Schedule 3 material of isochronal anneals of 1 h prior to post-deformation aging. Up to 1650°F (899°C), the hardness of the undeformed, rolled, and shocked states dropped by the same amount. The softening in this range was thought to be due to excessive growth and subsequent dissolution of  $\gamma''$ . While this is the recovery range, dislocation rearrangements would not have contributed significantly to the hardness decrease. Between 1650°F (899°C) and 1750°F (954°C), recrystallization occurred, causing the hardness of deformed material to decrease at a faster rate than that of the undeformed specimens. Beyond 1750°F (954°C), the hardness is independent of history.

The most important steps in the isochronal annealing process were confirmed optically. For example,

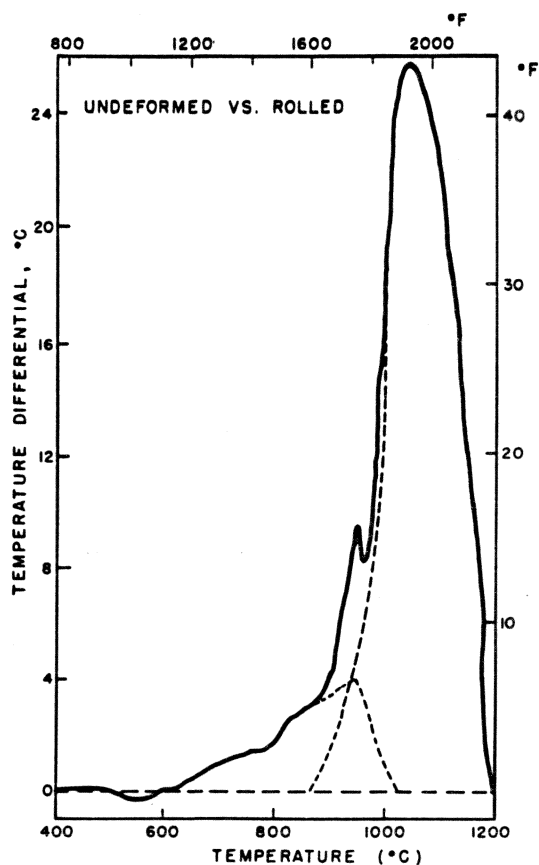


Fig. 8—Differential thermal analysis of the rolled vs undeformed conditions, with a predeformation age of 1300°F (704.4°C)/4 h (Schedule 3).

at 1700°F (927°C), evidence of recrystallization was observed and at 2000°F (1093°C), extensive grain growth had occurred for all three conditions; the average grain diameters were found to be essentially the same.

The shocked and rolled conditions of Schedule TMP-3, prior to post-deformation aging, were analyzed with reference to undeformed standards by means of differential thermal analysis. TMP-3 schedule was chosen because a substantial portion of  $\gamma''$  precipitation had already taken place. Therefore, differences in  $\gamma''$  precipitation kinetics would be less likely to interfere with the results. In the analysis of the data, the precipitation rate was assumed to be the same for the deformed and undeformed conditions, although it is known to depend on mechanical history.<sup>14</sup> In order to minimize this effect further, the highest possible rate of heating was used.

There were two striking features of the results shown in Figs. 8 and 9. Firstly, the shape of the energy release curves for rolled and shocked material was similar. Secondly, significantly more energy was released by the former than the shocked. Comparison

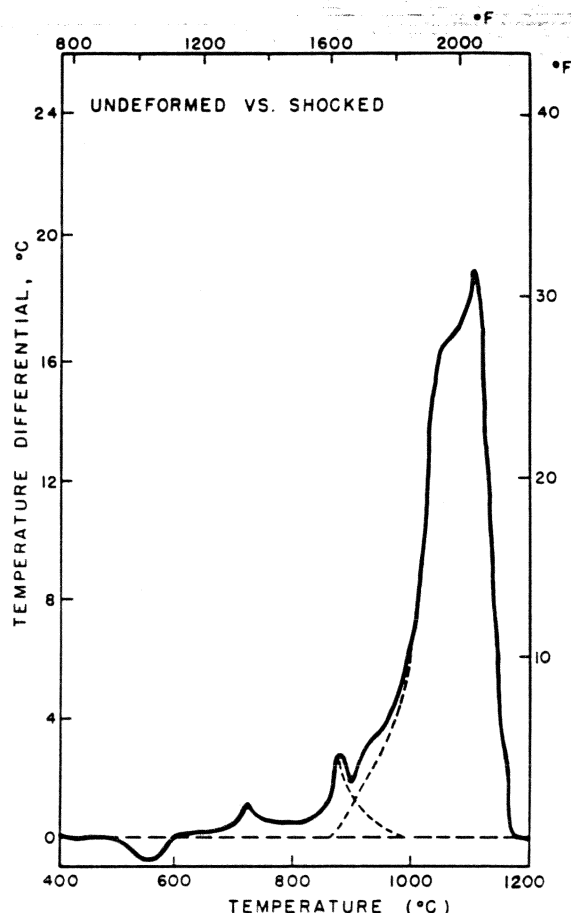


Fig. 9—Differential thermal analysis of the shocked *vs* undeformed conditions, with a predeformation age of 1300°F (704.4°C)/4 h (Schedule 3).

with previous findings,<sup>18,19</sup> coupled with hardness and metallographic observations, suggested that the irregular peaks between 1200°F (649°C) and 1700°F (927°C) were the result of recovery, while the much larger peaks near 1900°F (1038°C) were associated with recrystallization. The interpretation of the depressions in the vicinity of 1000°F (538°C), manifesting energy absorption, is open to speculation. They could be due to the disruption of vacancy-solute atom complexes. Alternatively, the anomaly could be associated with the formation of a structural change known as the “K-state”.<sup>20,21</sup> The higher energy release for rolled than for shocked material almost certainly reflects a higher dislocation density in the former.

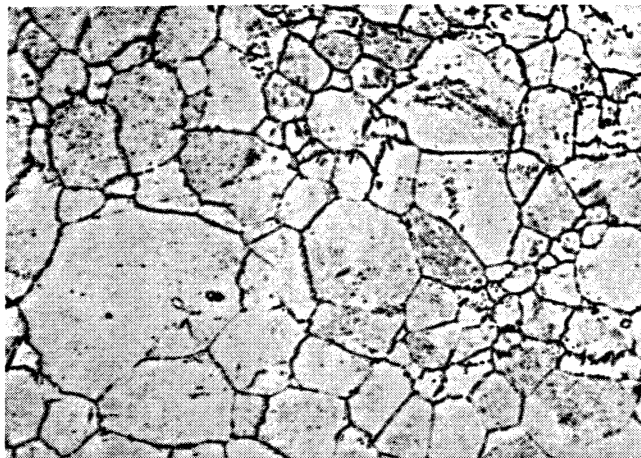
#### Thermal Stability

It is known that long anneals at 1400°F (760°C) induce the formation of the stable  $\delta$  phase and that rolling accelerates its occurrence. To evaluate the relative influence of shock straining and cold rolling, samples of material processed according to Schedules 3 and TMP-3 were annealed for 100 h at 1450°F (788°C). As demonstrated in Fig. 10, the undeformed condition had only minor amounts of platelike  $\delta$  phase, primarily at grain and twin boundaries. After TMP, however, precipitation of  $\delta$  was enhanced, being considerably finer in distribution and more extensive in shock-processed material. Although the above temperature exceeds normal

service temperatures, it might prove fruitful to investigate the impact of shock-deformation induced, finely distributed,  $\delta$  phase on alloy properties.

#### Substructure Strengthening Characteristics

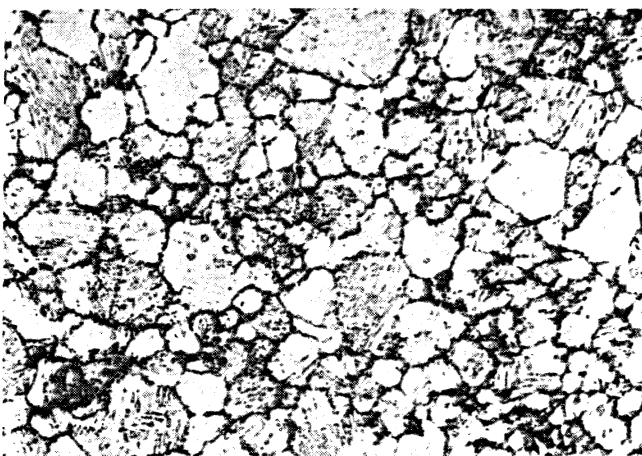
The true stress-true strain curves in Fig. 11 emphasize the effect of prestrain rate on tensile behavior.



(a)



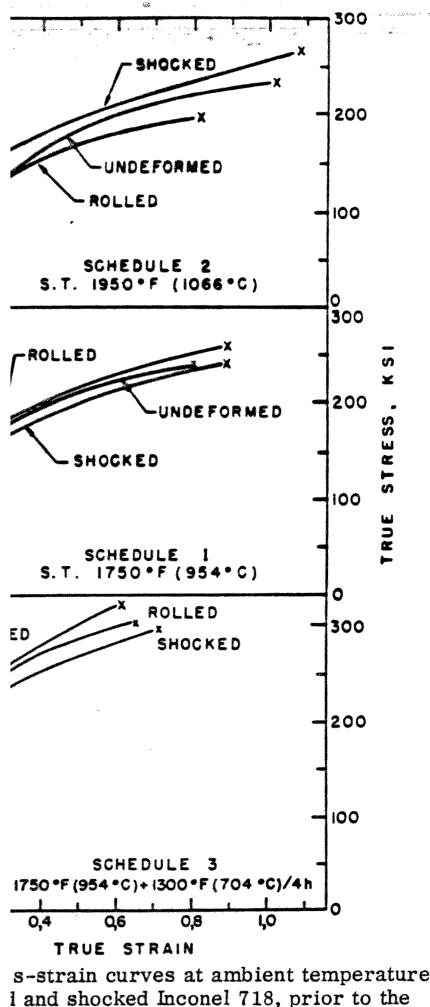
(b)



(c)

Fig. 10—100 h anneal at 1450°F (787.8°C) (magnification 500 times) for the predeformation age of 1300°F (704.4°C)/4 h (Schedule 3): (a) undeformed; (b) rolled; (c) shocked.





s-strain curves at ambient temperature  
1 and shocked Inconel 718, prior to the

deformed conditions reflect the 24 train imparted by cold rolling or evident that the effectiveness of creases as the basic, initial strengths.

## Fracture

rature tensile fractures of Schedule as were compared with those of ecimens, using optical and scanning y. The fracture mode was predom ar shear rupture, as shown in Fig. ere prevalent. Firstly, the dimples ctile fracture were associated with . Their size was approximately the and much larger than the  $\gamma''$  pre- cates that the initiation of fracture ociated with crack nucleation with- at the matrix-precipitate interface. s of the thermally-processed mate- re suggestive of a lower toughness. carbides were observed, indepen- story. Carbide fracture seemed to leavage. The particularly smooth, nce of the fracture surface of the MC carbide in Fig. 12(d) indicated probably initiated at the carbide it-

self. The fact that most of the carbides were cracked also pointed to the fact that they were responsible for the initiation of room-temperature failures.

## Synthesis

There is little doubt that the optimized Schedule, TMP-3, which led to improvements in overall properties well beyond those reported previously for Inconel 718, derives its superiority from the predeformation aging treatment. For Schedules TMP-1 and TMP-2, where strain is introduced in the solution treated condition, the majority of precipitation occurs during the final aging sequence. Consequently, nucleation of precipitates can take place on dislocations arranged primarily in planar arrays. This will yield a nonuniform dispersion of fairly large second-phase particles, with zones substantially devoid of precipitates in the vicinity of the slip bands. Another factor also interferes with the achievement of high strengths—the possibility of substructure recovery during the first postdeformation aging treatment.

The predeformation age in Schedule TMP-3 establishes a homogeneous precipitate distribution which is not disturbed significantly by subsequent slip. Thus, once worked, the alloy not only has a preexisting set of obstacles which inhibit thermal substructure recovery, but also a uniform distribution of nuclei. On further aging, these grow into a homogeneous dispersion of precipitates, thereby minimizing localized sources of weakness.

In the case of shock TMP, the above is coupled with the observed refinement of slip. Slip is still planar but the arrays are closer together. This finer dispersion of slip is fairly typical of shock-loaded materials. Shocked nickel, for example, exhibits a smaller cell size than conventionally strained nickel.<sup>22</sup> The short period ( $\sim 1$  ns) during which an initial plastic strain of about 10 pct must be accommodated enforces the operation of many more sources, with shorter dislocation segments moving shorter distances.

The refinement of slip can account for the tendency for shock TMP to yield a larger reduction in area and higher toughness index at lower temperatures than conventional TMP. If the origin of fracture is the MC carbides, then the higher stress concentration associated with the coarser slip bands in cold-rolled material will be more effective in aiding crack nucleation than finer bands in shocked material. One can also understand the presence of a more uniform dispersion of  $\delta$  phase in shock-processed specimens in terms of slip refinement.

The similarity in the shape of the DTA energy release curves indicates that the annealing response after conventional and shock TMP are both characterized by the three classical stages of recovery, recrystallization and grain growth. However, the relative heights of the peaks point to the fact that the dislocation density was higher in TMP-3R than TMP-3S material. This would help to explain the decrease in the effectiveness of shock hardening (compared to the cold-rolling response), as the initial strength of the alloy increases, in the partially aged, as deformed conditions (Schedule 3, Fig. 11).

The lower dislocation density in material processed according to TMP-3S, relative to TMP-3R, is thought

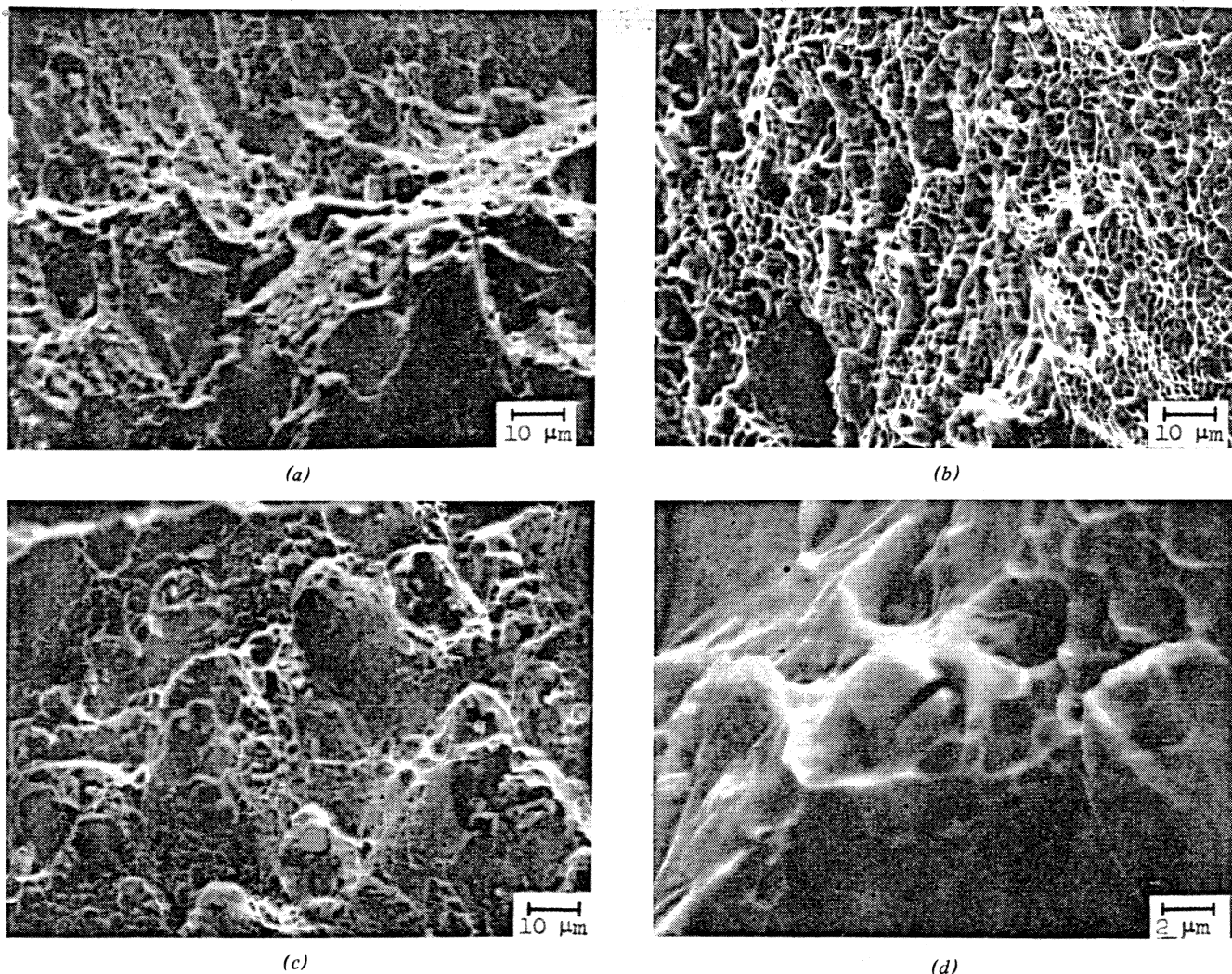


Fig. 12—Scanning electron fractographs of tensile fractures at ambient temperature: (a) Schedule 1—undeformed; (b) Schedule TMP-3R; (c) and (d) Schedule TMP-3S.

to reside in the fact that the maximum shear strain is a more realistic basis of comparison than the generalized or effective strain. The shear strain due to a 19.1 pct thickness reduction by cold rolling is 42.4 pct, contrasted with the 36.8 pct corresponding to a 510 Kbar shock wave. However, this argument appears to be a contradiction to the observations that shock-loaded pure metals have higher strengths, and higher dislocation densities, than conventionally deformed metals.<sup>22,23</sup> Also, the as-deformed behavior of Inconel 718 which was solution treated at the higher temperature falls into this category. (Schedule 2, Fig. 11). The explanation for this apparent paradox is believed to lie not so much in the dependence of shock substructure on initial material strength as it does in the response to deformation at lower strain rates.

Consider the influence of alloy strengthening on the relative contributions of dislocation density,  $\rho$ , and mean free path,  $\bar{s}$ , to the total shear strain,  $\gamma$  expressed as

$$\gamma = b\rho\bar{s} \quad [1]$$

As matrix strength increases due to solid solution (Schedule 1) and, particularly, precipitation hardening (Schedule 3), there will be a tendency for  $\bar{s}$  to de-

crease. Therefore,  $\rho$  must be higher in order to accommodate a given applied strain. Thus, since  $\bar{s}$  is already quite limited during shock straining, the disparity in dislocation density between cold-rolled and shock-loaded material will be reduced as predeformation strength increases. Eventually, then, the precise method of strain comparison becomes important and distinguishable.

The higher strengths resulting from the TMP-3R than TMP-3S optimized schedules can be understood now in terms of the following factors. Firstly, the contribution of substructure to strengthening is higher in TMP-3R. Secondly, predeformation aging serves to minimize differences in final dislocation and precipitate distributions, and concomitant strength differences. In Schedules TMP-1 and TMP-2, where working is performed in the solution treated condition, the dispersion of heterogeneously nucleated second phase is finer in shock-processed material because the dislocation substructure is finer and more evenly distributed.

However, in Schedule TMP-3, the predeformation age reduces the prestrain-rate effect because the pre-existing homogeneous distribution of precipitate nuclei serves two major purposes. As discussed previously,

it impedes thermal recovery during final aging, and results in the development of a uniform precipitate distribution in fully-processed material. In addition, it also controls and refines the scale of slip during cold rolling—a factor less important in the case of shock loading because the distribution is maintained on a fine scale by the high rate of strain. Any subsequent homogeneous nucleation on dislocations during final aging would not lead then to a particularly coarse, widely-spaced secondary precipitate. While the slip band spacings in TMP-3R are larger on the average than in TMP-3S, the density, between the bands, of dislocations stabilized by second phase is higher, and their distribution finer than in TMP-1R or TMP-2R. Thus, it is postulated that the difference in strength between TMP-3R and TMP-3S is attributable to a difference in dislocation density; the disparity in final dislocation and precipitate distributions is insufficient to provide a significant contribution.

## SUMMARY AND CONCLUSIONS

The principal results of this investigation and the conclusions drawn therefrom may be summarized as follows:

- 1) Thermomechanical processing (TMP) utilizing cold working is an effective method of improving the properties of Inconel 718 nickel base superalloy.
- 2) Inconel 718 was thermomechanically processed successfully by shock loading to a peak pressure of 510 Kbar or cold rolling to a thickness reduction of 19.1 pct—an equivalent generalized or effective strain.
- 3) TMP is substantially more effective when strain is imparted in the partially aged than in the solution treated condition. The best sequence of thermal and mechanical treatment conditions was found to be:

Solution Treatment: 1750°F (954°C), 1 h, AC  
 Predeformation Age: 1300°F (704°C), 4 h, AC  
 Cold Work  
 Final Age: 1250°F (677°C), 8 h, FC in 1 h to 1150°F (621°C), total 18 h.

- 4) With this schedule of treatments, conventional and shock TMP led to improvements in room and elevated temperature strength and low-cycle fatigue life, and in stress-rupture life at 1000°F (538°C) and 1200°F (649°C); toughness and ductility were enhanced for some testing conditions and decreased minimally in others.

For example, room temperature strengths in excess of 230 Ksi (1590 MN/m<sup>2</sup>) were achieved by conventional and shock TMP (using a double shot). Conventional TMP led to a 1000 h rupture strength at 1000°F (538°C) greater than 170 Ksi (1170 MN/m<sup>2</sup>), and shock TMP nearly doubled the rupture life at 1200°F/110 Ksi (649°C/758 MN/m<sup>2</sup>).

- 5) The beneficial effect of predeformation aging was thought to reside with the establishment of a uniform distribution of  $\gamma''$  precipitate nuclei which is not disturbed during subsequent cold working. During final aging, the preexisting precipitates impede thermal substructure recovery, and grow into a homogeneous distribution of fine, second-phase particles. Moreover, the nuclei serve to control and refine the scale of slip during working. Therefore, the size and dis-

persion of precipitates heterogeneously nucleated thereafter would not depart significantly from those of the primary, homogeneously nucleated precipitates.

- 6) The effects of conventional and shock TMP was compared on the basis of equivalent generalized strain. The higher dislocation density in the former led to the conclusion that maximum shear strain is a more valid basis of comparison.

- 7) The higher strengths of conventionally-processed material when the above thermal treatment parameters were used can be accounted for in terms of its higher dislocation density; predeformation aging minimizes the dependence of strength on working rate, which might normally arise from differences in dislocation and precipitate distribution.

- 8) Since property modifications in Inconel 718 due to TMP are associated primarily with substructure strengthening, thermal recovery sets a realistic limit of 1200°F (649°C) on the temperature beyond which such processing, irrespective of the method of working, is no longer an effective strengthening technique.

- 9) Room-temperature fracture of unnotched tensile samples took place by transgranular shear rupture for the standard undeformed and optimized TMP conditions. The initiation of failure seems to be connected to the fracturing of the massive MC carbides.

While the interpretation provided herein of the response of Inconel 718 to TMP appears to be relatively self-consistent, much of it is recognized to be speculative and subject to different points of view. Undeniably, further studies are required to improve our understanding of the observed phenomena, particularly at lower shock strains to permit better TEM resolution of dislocations. Nevertheless, it has been shown that TMP utilizing explosive shock loading is a viable method for enhancing the overall mechanical behavior of this alloy.

## ACKNOWLEDGMENTS

This work was performed at the Denver Research Institute, University of Denver, Denver, Colorado. The authors are indebted to the U. S. Naval Air Development Center, Department of the Navy, for financial support under contract No. N62269-73C-0376, and to the Coordenação de Aperfeiçoamento de Pessoal de Nível Superior for the award of a fellowship to one of us (M.A.M.) while a graduate student at the University of Denver.

The assistance of Mr. Davis Carpenter, making possible the use of the differential thermal analysis apparatus, is gratefully acknowledged.

## REFERENCES

1. W. H. Coats, Jr. and J. E. Coyne: *Proc. 2nd Conf. on Superalloys*, Chapter K, Report No. MCIC-72-10, Metals and Ceramics Information Center, Battelle Memorial Institute, Columbus, Ohio, 1972.
2. C. J. Slunde and A. M. Hall: NASA TMX-53443, Battelle Memorial Institute, Columbus, Ohio, 1966.
3. B. H. Kear, J. M. Oblak, and W. A. Owczarski: *J. Metals*, 1972, vol. 24, no. 6, pp. 25-32.
4. F. M. Richmond: *J. Eng. Power*, 1967, vol. 89, pp. 61-74.
5. R. S. Cremisio, H. M. Butler, and J. F. Radavich: *J. Metals*, 1969, vol. 21, no. 11, pp. 55-61.
6. R. F. Decker: *Steel-Strengthening Mechanisms*, pp. 147-70, Climax Molybdenum Co., 1969.

7. J. C. Uy, C. J. Nolan, and T. E. Davidson: *Trans. ASM*, 1967, vol. 60, pp. 693-98.
8. R. N. Orava: *Mater. Sci. Eng.*, 1973, vol. 11, pp. 177-80.
9. R. N. Orava: Denver Research Institute, University of Denver, Final Report No. DRI 2638, Contract No. N62269-73-C-0376, U.S. Naval Air Systems Command, 1974.
10. M. A. Meyers: Ph.D. Dissertation, University of Denver, Denver, Colorado, 1974.
11. H. J. Wagner, R. S. Burns, T. E. Carroll, and R. C. Simon: *Nickel-Base Alloys/Alloy 718*, Defense Metals Information Center, Battelle Memorial Institute, Columbus, Ohio, 1968.
12. M. Conserva, M. Buratti, E. Di Russo, and F. Gatto: *Mater. Sci. Eng.*, 1973, vol. 11, pp. 103-12.
13. R. A. Heacock: *Proc. 2nd Intl. Conf. on Superalloys*, Chapter P, Report No. MCIC-72-10, Metals and Ceramics Information Center, Battelle Memorial Institute, Columbus, Ohio, 1972.
14. A. Kaufman and S. Niedzwiedz: *Proc. of the Conference on Quantitative Relation Between Properties and Microstructures*, Israel University Press, 1969, pp. 139-44.
15. J. P. Stroup and R. A. Heacock: *J. Metals*, 1969, vol. 21, no. 11, pp. 46-54.
16. D. R. Muzyka and G. N. Maniar: *Metals Eng. Quart.*, 1969, November, pp. 23-36.
17. C. S. Smith: *Trans. TMS-AIME*, 1958, vol. 212, pp. 574-89.
18. L. M. Clarebrough, M. E. Hargreaves, and G. W. Est: *Proc. Roy. Soc., London*, 1955, vol. 232A, pp. 252-70.
19. R. W. K. Honeycombe: *The Plastic Deformation of Metals*, pp. 289-300, St. Martins Press, New York, 1968.
20. H. E. McCoy, Jr. and D. L. McElroy: *Trans. ASM*, 1968, vol. 61, pp. 730-41.
21. A. Christou and N. Brown: *Phil. Mag.*, 1973, vol. 27, pp. 281-96.
22. R. L. Nolder and G. Thomas: *Acta Met.*, 1964, vol. 12, pp. 227-40.
23. G. E. Dieter: *Response of Metals to High Velocity Deformation*, P. G. Shewmon and V. F. Zackay, eds., pp. 409-45, Interscience, New York, 1961.